INTERFACE

royalsocietypublishing.org/journal/rsif

Research

Cite this article: Orndorf N, Garner AM, Dhinojwala A. 2022 Polar bear paw pad surface roughness and its relevance to contact mechanics on snow. *J. R. Soc. Interface* **19**: 20220466.
https://doi.org/10.1098/rsif.2022.0466

Received: 23 June 2022
Accepted: 11 October 2022

Subject Category:
Life Sciences–Physics interface

Subject Areas:
biomechanics, biomimetics, biophysics

Keywords:
ecomorphology, paw pads, surface roughness, contact mechanics, friction, snow

Author for correspondence:
Ali Dhinojwala
e-mail: ali4@uakron.edu

†Present address: Department of Biology and BioInspired Institute, Syracuse University, Syracuse, NY 13244, USA.

Electronic supplementary material is available online at https://doi.org/10.6084/m9.figshare.c.6260159.

THE ROYAL SOCIETY PUBLISHING

Polar bear paw pad surface roughness and its relevance to contact mechanics on snow

Nathaniel Orndorf[1], Austin M. Garner[2,†] and Ali Dhinojwala[1]

[1]School of Polymer Science and Polymer Engineering, and [2]Integrated Bioscience Program, Department of Biology, The University of Akron, Akron, OH 44325, USA

NO, 0000-0003-4977-5790; AMG, 0000-0003-1053-9168; AD, 0000-0002-3935-7467

Microscopic papillae on polar bear paw pads are considered adaptations for increased friction on ice/snow, yet this assertion is based on a single study of one species. The lack of comparative data from species that exploit different habitats renders the ecomorphological associations of papillae unclear. Here, we quantify the surface roughness of the paw pads of four species of bear over five orders of magnitude by calculating their surface roughness power spectral density. We find that interspecific variation in papillae base diameter can be explained by paw pad width, but that polar bear paw pads have 1.5 times taller papillae and 1.3 times more true surface area than paw pads of the American black bear and brown bear. Based on friction experiments with three-dimensional printed model surfaces and snow, we conclude that these factors increase the frictional shear stress of the polar bear paw pad on snow by a factor of 1.3–1.5 compared with the other species. Absolute frictional forces, however, are estimated to be similar among species once paw pad area is accounted for, suggesting that taller papillae may compensate for frictional losses resulting from the relatively smaller paw pads of polar bears compared with their close relatives.

1. Introduction

Understanding the structure–function relationship of biological materials is critical for enhancing our understanding of the natural world and creating biomimetic materials. Over millions of years, many biological systems have adapted to varying environmental demands and thus exhibit variation in form that relates to effective functioning in particular habitats. Not surprisingly, such systems have been primary targets for technological inspiration and innovation via biomimicry. One often-examined system is the adhesion of various biological organisms to ecologically relevant substrates. Much work has been done to understand the physical and chemical mechanisms behind the microstructure adhesive systems of lizards [1–10], frogs [11–14], insects [15–20] and underwater organisms [21–25]. However, despite evolving in a myriad of environmental conditions, the structures on mammalian paw pads in the context of traction on ecologically relevant substrates has not received much attention. An often-cited example in the biomimetics literature is the assertion that the surface roughness of the paw pads of the polar bear (*Ursus maritimus*) is adapted to improve friction on ice and snow. However, this assertion is predicated on a single morphological study conducted in the mid-1980s. Manning *et al.* examined the microstructures on a paw pad of a polar bear, noted raised papillae and depressions with diameters of about 1 mm, and suggested the structures to be adaptive traits that increase traction on ice [26]. This suggestion has undoubtedly led to the desire of researchers to mimic the microstructures of the paw pads of polar bears to design materials with enhanced traction on ice and snow (e.g. winter tyres and shoe soles) [27]. However, Manning *et al.* made no morphological comparisons with other bear species, nor did they make measurements or predictions of friction between

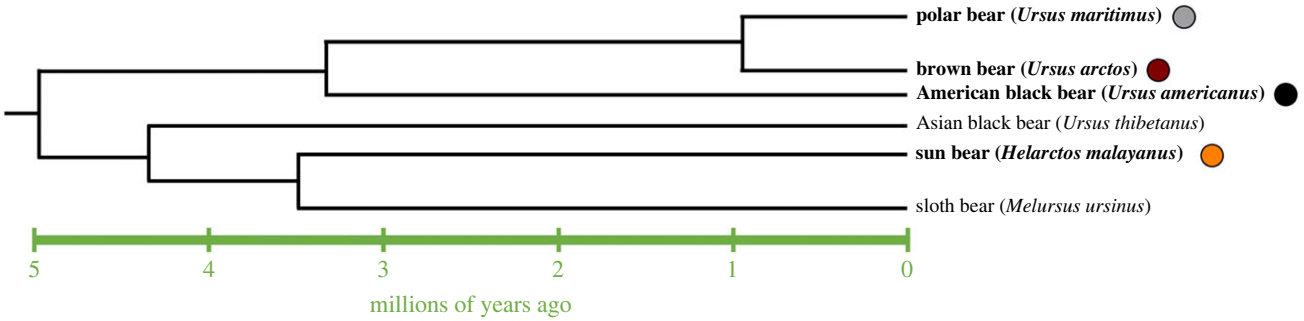

Figure 1. Phylogenetic tree of the bear subfamily Ursinae, adapted from [32]. The species used in this study are listed in bold, and the colour represents their respective colours in the plots throughout the text.

the paw pads and ice or snow. Interestingly, at least one study published prior to Manning *et al*. describes small papillae on the surface of American black bear (*Ursus americanus*) paw pads [28], yet no comparative studies on the paw pad surface roughness or morphology have been published. Thus, it is unclear whether the surface roughness of the paw pad of the polar bear actually contributes to an improvement of friction on ice or snow. Despite this shortfall, the assumption that papillae help polar bears maintain traction on ice and snow is thoroughly accepted in the literature, textbooks and general media [29–31].

The bear subfamily Ursinae (figure 1) exploits a considerable variety of habitats and, not surprisingly, possesses a number of traits that purportedly allow effective functioning in such environments. Malayan sun bears (*Helarctos malaynus*) and black bears, for example, typically inhabit forested areas, as they climb trees for feeding, shelter and safety [33,34]. These species of bear have a number of morphological features that aid in effective climbing, including well-developed hindlimb muscles [35]; longer phalanges [36]; sharply curved claws [36]; short metatarsals [36]; and wrinkled, largely naked paw pads [28]. In contrast, terrestrial bears, such as brown bears (*Ursus arctos*) and polar bears, have less well-developed hindlimb musculature [35], short phalanges [36], long hindlimbs [36], and less wrinkles and more fur on their paw pads [33].

Although polar bears and brown bears are both terrestrial, there are morphological differences on their paws related to their different habitat and terrain [32]. Polar bears adapted to live on the Arctic sea ice [32] and correspondingly have smaller paw pads with greater fur coverage on the paws [37] and short, sharp claws [29,38]. Decreased paw pad size in exchange for furred areas decreases the amount of heat loss in their cold habitats [37], and is also observed in other snow-dwelling animals [39–43]. In addition to thermal stability, paw fur will probably differentially influence traction on different substrates, yet this effect has not been studied. Although polar bear claws are shorter and more curved than those of brown bears, polar bear paw prints rarely show claw marks [29,38], suggesting that they do not generally rely on their claws to provide grip on snow.

A critical assumption in Manning *et al.*'s conclusions is that polar bears excel at walking on ice and snow relative to other species, yet direct evidence of this is absent in the literature. Brown bears and polar bears have the same energetic cost of locomotion on a treadmill [44], but no studies have quantitatively compared their efficiency on different substrates. In a qualitative observational study, polar bears walked easily on a slippery polymer surface, while brown bears were hesitant to attempt to walk on it [38]. Additionally, polar bears left the same footprints on the slippery and natural surfaces [38]. To the contrary, footprints of brown bears differ on moist soil than mud and snow; in moist soil, their prints are typically smaller than their paw pad size, but in mud and snow their prints are typically larger than their paw pad size [45]. These observations suggest that brown bears' paws slide on mud and snow, but polar bears are able to walk easily on slippery surfaces. Potential explanations for this observation can come from a combination of differences in running mechanics [38,46–48], paw sizes [49–51] and paw pad microstructures [26].

Here, we examine the surface roughness of the paw pads of several preserved species of bear. Specifically, we quantify the surface roughness at length scales from 1 cm down to 100 nm by computing the surface roughness power spectral density of the paw pad surfaces. In conjunction with the morphological characterization, experimental friction results of model surfaces on snow are used to make predictions of relative frictional stresses of the paw pads on snow, which is the main contact between polar bear paws and their habitat [52].

2. Experimental methods

2.1. Samples

In total, 13 individual organisms were studied including five polar bears, four brown bears, three American black bears and one sun bear. These individuals contain samples with various forms of preservation, including ethanol preservation, frozen samples and taxidermy. Ethanol-preserved polar bear paws from one individual were acquired from The University of Alaska's Museum of the North (UAM138220), along with frozen black bear cub paws from one individual (UAM138221). Frozen black bear paws from another organism were acquired from a private taxidermist. Taxidermied sun bear paws from one organism were obtained from the Akron Zoo, which were used to make surface replicas (Microset 101RT, Microset Products Ltd) for examination. The samples from the remaining nine individual organisms consist of surface replicas of paw pads of taxidermy exhibits in private collections. Microset 101RT produces surface replicas with a resolution of 0.1 µm. All samples other than the frozen samples were fixed (typically with a formaldehyde) so degradation of the structures is unlikely. The frozen samples were frozen and analysed within a few weeks of the organisms' death. On all available samples, the paw and paw pad widths and lengths were measured as the longest dimension of the paw/pad in its respective direction.

Figure 2. Paws of each of the bear species studied: polar bear hind and forepaw (*a*), brown bear forepaw (*b*), American black bear fore and hind paw (*c*, with paw pad samples removed), sun bear forepaw (*d*) and sun bear hind paw (*e*). The polar bear paws have much more fur than the other species'. The sun bear paw pads are deeply wrinkled, the black bear paw pads are less wrinkled, and the brown bear and polar bear have very few wrinkles. The polar bear, brown bear and black bear paw pads have papillae, but the sun bear paw pads do not.

2.2. Papillae size measurements

On all samples, the average papilla base diameter was measured. For the ethanol preserved and frozen samples, samples were cut from the paw pad (figure 2*c*) and both optical microscopy and scanning electron microscopy (SEM) were used to image and measure papillae base diameter on several areas of the sample from which an average was calculated. Due to the optical properties of the surface replica material, the replicas of taxidermied paw pads were unable to be examined using optical microscopy, so stylus profilometry was used with a tip radius of 2 µm. The average papillae base diameters of the surface replicas were measured by assuming that a single papillae diameter D exists and calculating it based on the average intercept length l of the profilometry scan across the papillae.

$$D = \frac{4l}{\pi}. \tag{2.1}$$

This is the same method certified by ASTM International (American Society for Testing and Materials provides standards across all disciplines) to measure the average grain size of metals [53], and has also been used for ice [54]. For one black bear sample, both measurement methods were used in order to confirm the agreement of results between methods. Stylus profilometry was also used to measure the root-mean-square height (h_{rms}) of each replica sample. The value of h_{rms} is directly proportional to the average papillae height, and thus is used to approximate the relative height of the papillae.

2.3. Power spectral density

Stylus profilometry was also used to examine the smaller length scale roughness of the surface replicas down to the material's resolution (0.1, µm) using a 200 nm tip. In order to determine the amplitude of roughness at any given length scale, the power spectral density function (PSD) is used. The PSD describes the amplitude of the surface roughness at each wavevector $q = 2\pi/\lambda$ where λ is the periodicity of the roughness profile [55]. The advantage of the PSD is that it can be used to calculate the contribution to macroscopic surface parameters from a specific range of length scales. For example, the PSD can be used to calculate common surface roughness parameters (e.g. RMS height, h_{rms}) between certain biologically relevant length scales (as defined by a minimum and maximum wavevector q_{min} and q_{max}). Similarly, the PSD can be used to calculate surface area parameters between minimum and maximum wavevectors. The addition of surface roughness to an otherwise flat surface results in an increase in total surface area (referred to as the true surface area, A_t). The relative magnitude of the increase in surface area resulting from surface roughness can be calculated via the ratio of A_t to the surface area assuming a completely flat surface (referred to as the apparent surface area, A_0) [56]. Details of these calculations are given in the electronic supplementary material.

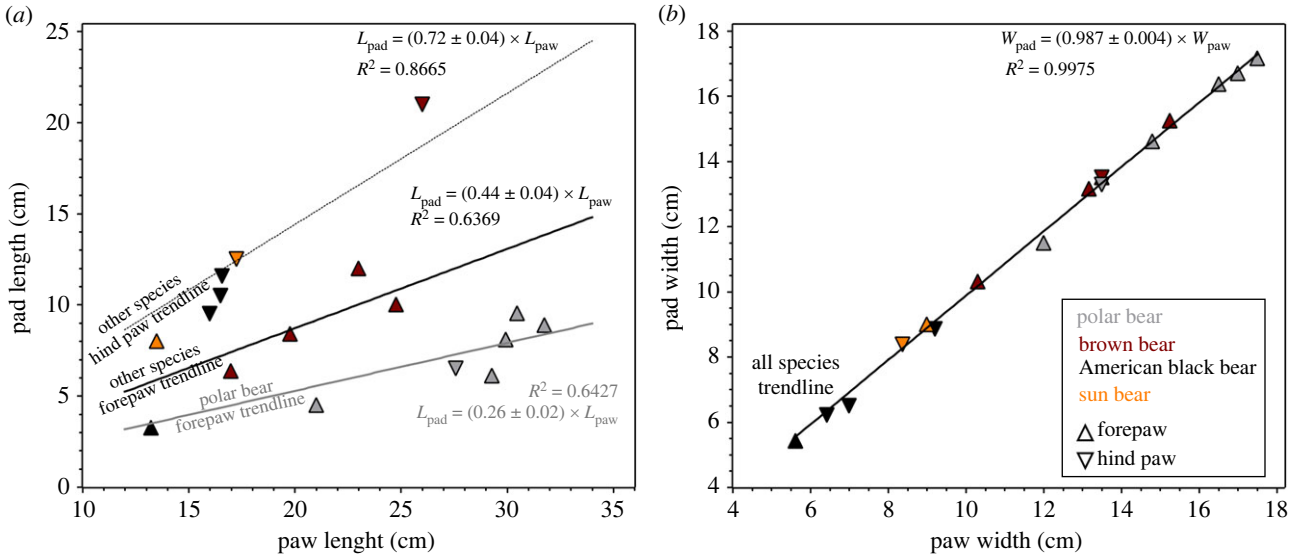

Figure 3. How the size of the paw pads scales with paw size for various bear species. Both hind and forepaw pad lengths of the polar bear are smaller than other species' with similar paw lengths (*a*), but the hind and forepaw pad widths of all species is nearly identical at similar paw widths (*b*). Each data point represents an individual organism.

2.4. Model surfaces

To replicate the papillae on bear paw pads, three-dimensional 20 × 20 × 4 mm sinusoidal surfaces were fabricated with a Formlabs Form 2 Stereolithography three-dimensional printer using Standard Black Resin with a layer resolution of 25 µm . The cured Standard Black Resin has an elastic modulus of approximately 2 GPa and a water contact angle of 65°. A total of nine surfaces were made by varying both the diameter (wavelength) and height (2 × amplitude) of the structures with values of 0.50, 1.25 and 2.00 mm. The finished surfaces were rinsed in isopropyl alcohol and air dried before the friction experiments to ensure that all uncured resin was removed.

The static frictional force between each surface and snow was measured using a laboratory-built friction apparatus and cooling stage (schematic in electronic supplementary material). The friction apparatus consists of a Vernier Dual-Range Force Sensor attached to a stepper motor so that the force sensor can move along two axes (shear and normal). A Teflon sample probe was made to attach to the force sensor and hold the model surfaces for testing. A dish was attached to the top of the liquid nitrogen-controlled cooling stage (held at −20°C) to hold snow, which was made using a ZENY 300W Electric Ice Shaver. The model surface was pressed into the snow at a normal stress of 10 N cm^{-2} (see electronic supplementary material). Similarly, the area directly in front of the surface was compressed at the same normal stress using a piece of smooth Teflon which was then removed. The stepper motor was driven forward at 2 mm s^{-1} and the maximum shear force was recorded. Each surface was tested five times with fresh snow and the average force for each surface was divided by the apparent surface area to calculate the shear frictional stress.

3. Results

3.1. Paw pad and papillae size

Representative images of the paw of each bear species studied are shown in figure 2. As previously reported, polar bear paws have much more fur than those of the other species. To quantify this observation, figure 3 shows the relationship between the paw and paw pad size for all of the organisms studied. Figure 3*a* shows that the paw pad length of the polar bear hind and forepaw are much smaller than those of the other species with a similar paw length. Linear trends for the forepaw pad length of polar bears and the other three species are calculated separately. No trend is shown for polar bear hind paw because only a single data point was acquired. Figure 3*b* shows a similar plot for the width of the paws and paw pads. As apparent from figure 2, the paw pads of all species extend to nearly the edge of the paws, so the trend line in figure 3*b* is calculated with both the hind and fore paw of all four species. This shows that the width of the paw pads of all four species is nearly identical once the paw width is taken into account. Approximating the paw pads as rectangles, their area as a percentage of the total paw area can be calculated by multiplying the trend lines in figure 3*a*,*b*. Taking the ratio of the areas of the paw pad of the polar bear to that of the other species gives an approximation for the size of the polar bear paw pads compared with the other species' when the paw size is controlled for. Doing so shows that the forepaw pad area of polar bears is 1.7 ± 0.2 times smaller than that of the other species, while for the hind paw, it is approximately 3 times smaller.

Papillae are present on the paw pads of the three North American species, however, not on the sun bear's. Closer examination of the polar bear and black bear paw pads with SEM reveals the same papillae and depressions as reported on polar bears by Manning *et al*. (figure 4) [26]. Representative profilometry scans are shown in figure 5, which show both papillae and wrinkles.

Figure 6*a* shows the average papillae base diameter for each individual studied as a function of its paw pad width. Although the papillae tend to be larger on polar bears than the other species, the trend is almost completely accounted for based on paw pad size. Figure 6*b* compares each organism's paw pad h_{rms} with its average papillae base diameter. Interestingly, the polar bear paw pads show a higher h_{rms}

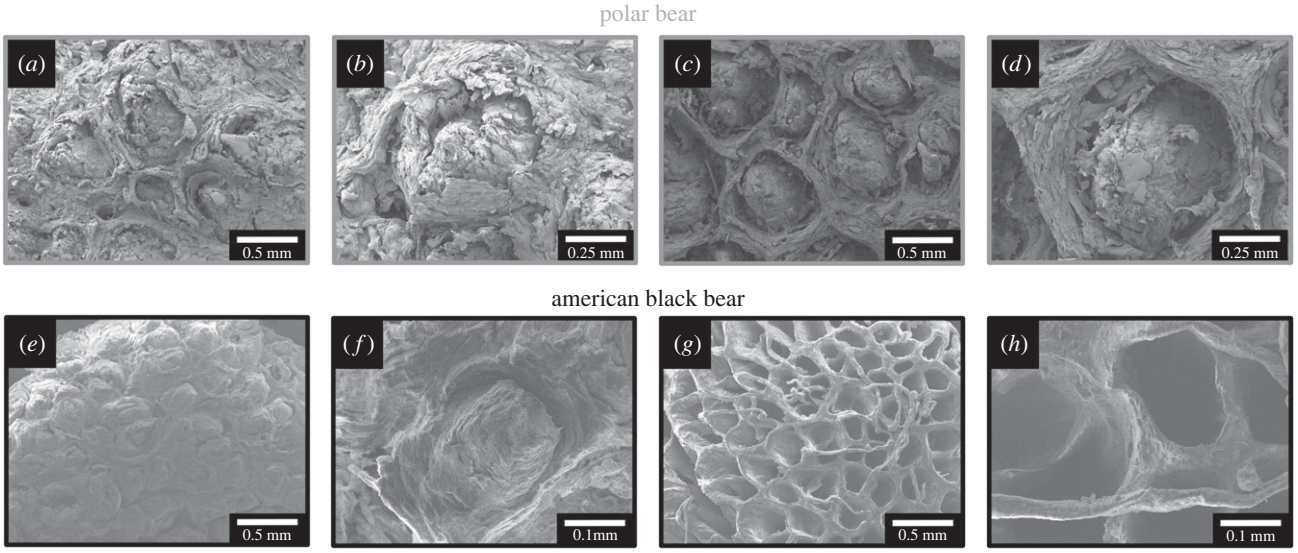

Figure 4. Scanning electron microscope images of the polar bear (*a–d*) and American black bear (*e–h*) paw pads show both raised papillae (*a*,*b*,*e*,*f*) and depressions (*c*,*d*,*g*,*h*).

than what would be expected from the trend of the other species. When the average papillae base diameter is controlled for, the polar bear papillae are 1.50 ± 0.08 taller than those of the brown bears and black bears.

3.2. Paw pad power spectral density

Figure 7 shows the average PSD for the four species studied. At most length scales, there are no large differences. However, small differences in the amplitude of the PSD may result in significant differences in contact mechanics. At smaller length scales, polar bear paw pads appear to be less rough than the other North American species.

The cumulative values of h_{rms} as smaller length scales of roughness are included for each species as calculated from the PSDs are shown in figure 8*a*. As expected, the larger length scales (smaller wavevectors) determine the overall values of h_{rms}. Black bears and brown bears have a nearly identical h_{rms}, while polar bears and sun bears do as well. Figure 8*b* shows the slope of the curves in figure 8*a*. A peak, or increase, in the slope helps determine which length scales contribute to h_{rms} the most. Sun bears show the most contribution to h_{rms} at the length scale of the wrinkles ($q \approx 10^3$ m^{-1}), meaning that its deep paw pad wrinkles result in a high h_{rms}. The three North American species all have peaks in the range of the papillae size ($q \approx 6 \times 10^3$ m^{-1}), showing that the papillae significantly contribute to their h_{rms}. The polar bear paw pads have an average h_{rms} that is 1.68 ± 0.05 higher than the brown and black bears' (without accounting for paw pad size).

The ratio of true surface area to apparent surface area is shown in figure 9 as a function of the maximum wavevector included. As more length scales of roughness are included in the calculation, the higher the area ratio becomes. Polar bears show the largest increase, while brown bears and black bears show about the same trend and sun bears show the smallest increase. The vastly different area ratio of polar bears and sun bears while having a similar h_{rms} shows the advantage of using the PSD to understand roughness at all length scales. All four species have two regions with high slopes, as shown in figure 9*b*. All four species show a peak in the slope in the length scale of the papillae ($q \approx 10^4$ m^{-1}). However, polar bears show the largest slope, showing that the taller papillae with similar base diameters creates more surface area. The peak in the papillae range for the sun bear is probably from wrinkles near the same length scale. The three North American species show another increase in slope around $q \approx 10^6$ m^{-1}, which corresponds to roughness on the papillae. Again, polar bears show the highest slope with the other two species being about the same. In total, the polar bear paw pads have a 1.33 ± 0.03 times higher area ratio than the brown and black bear paw pads. However, unlike h_{rms}, the area ratio is independent of the paw pad size (electronic supplementary material, figure S1).

3.3. Friction of model surfaces on snow

Representative images of the three-dimensional printed model surfaces are given in figure 10*a*. By decreasing the structure diameter D, the total number of structures on a single model surface increases.

The friction measurements show that both increasing the structure height and decreasing the structure diameter increases the shear frictional stress on snow (electronic supplementary material, figure S2A). Figure 10*b* shows a direct proportionality between the shear stress and H/D. The failure mechanism of each model surface is categorized as one of three modes: fracture, where all of the repeats had the majority of the surface cavities filled with snow after failure; slip, where there was no snow remaining in the cavities; or mixed, where either some of the cavities had snow remaining or some repeats showed a fracture mode and others showed a slip mode.

4. Discussion: relevance to contact mechanics on snow

The presence of papillae on the paw pads of all three North American bear species suggests that papillae themselves are not adaptations for increased traction on snow. The strong relationship ($R^2 = 0.9081$) between the papillae base diameter and paw pad width for all species also suggests that the lateral size of the papillae are not adaptations to snow. However, the average polar bear has papillae that are 1.68 ± 0.05 times taller than average brown and black bears.

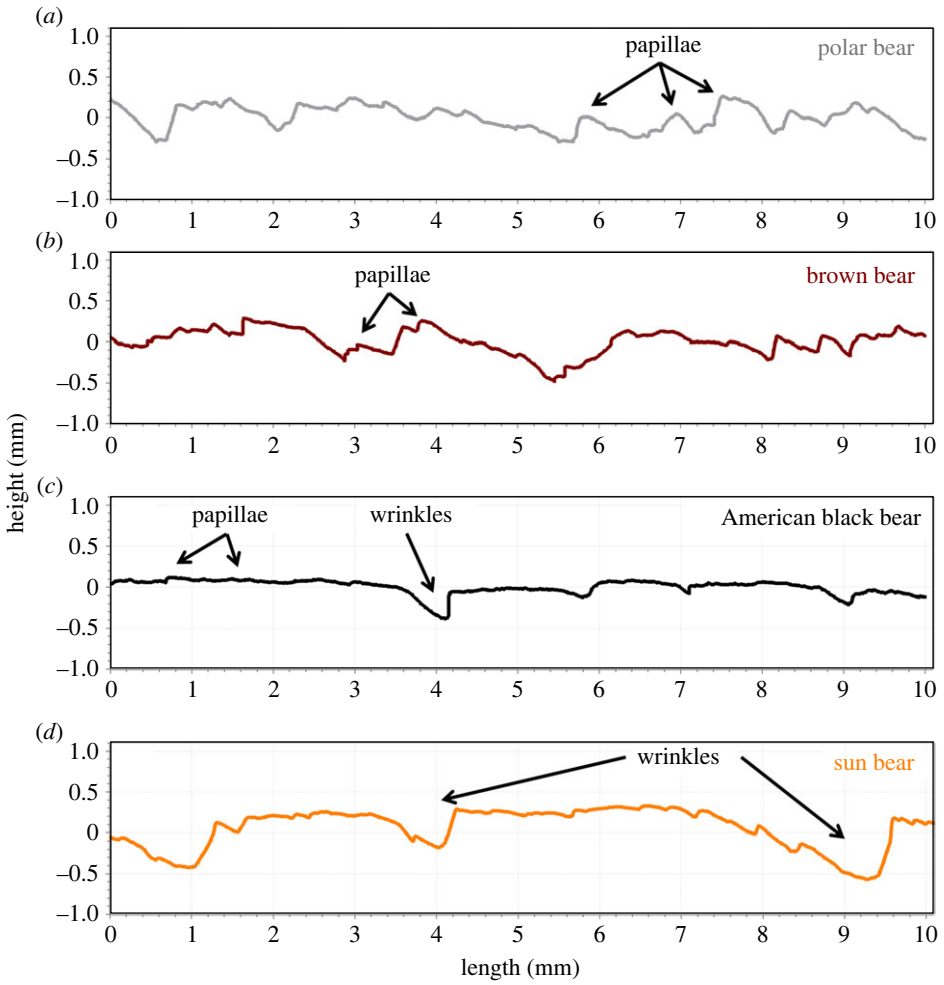

Figure 5. Representative stylus profilometry line scans of a polar bear (*a*), brown bear (*b*), American black bear (*c*) and sun bear (*d*). All plots are set at the same horizontal and vertical scale.

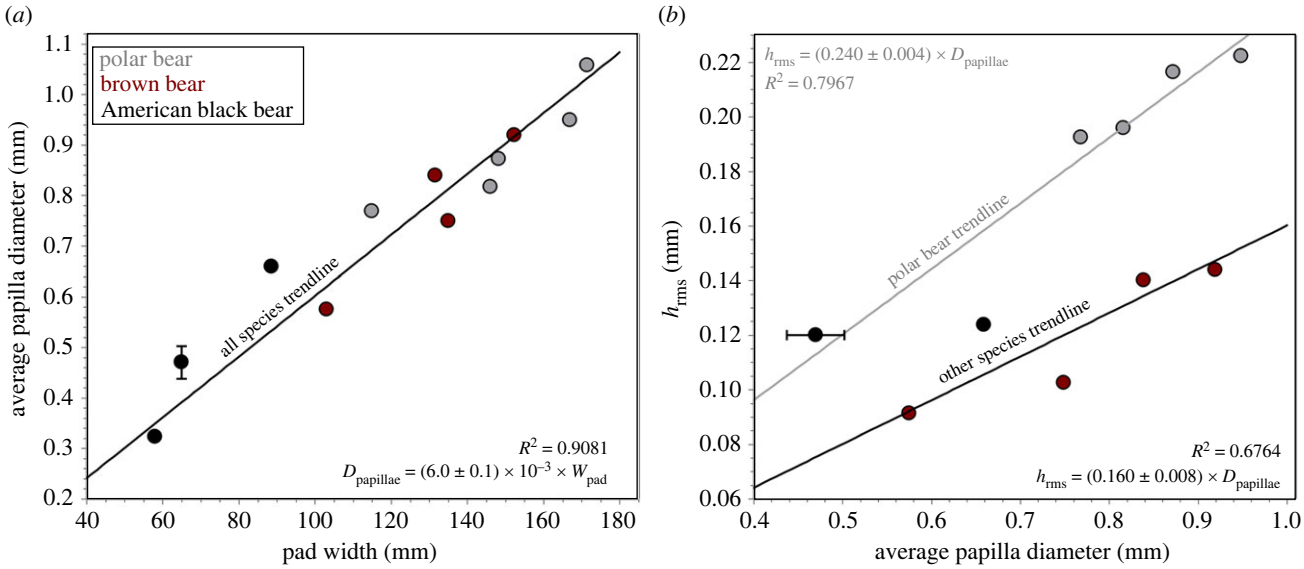

Figure 6. The base diameter of the papillae on the paw pads of the North American bear species can be explained by variations in the paw pad width (*a*). However, the papillae are taller on the polar bear paw pad evidenced by a higher h_{rms} (*b*). Each data point represents the average for a single individual. The error bar represents the difference in measurements made from optical microscopy on frozen paw pads and stylus profilometry on surface replicas of the same paw pads.

When the papillae base diameters (or pad widths) are scaled to the same size, the papillae height is 1.50 ± 0.08 times larger on polar bears than the other species, suggesting that taller papillae may be an adaptation for traction on snow. Figure 9*b* shows that the majority of the 1.33 ± 0.03 times as much true surface area on the polar bear paw pad is a result of their taller papillae, but that additional area comes from smaller length scales too. The contribution from the smaller length scale suggests that a possible mechanism for increasing traction on snow may not be solely increasing papillae height, but increasing contact area as well. While polar bears have a higher area ratio at the resolution of the

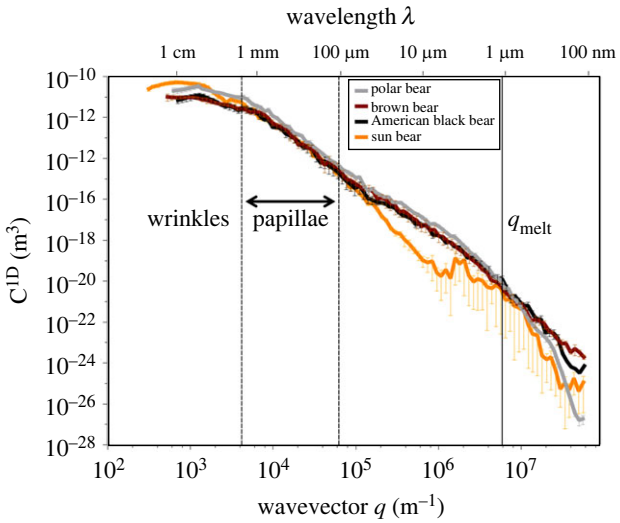

Figure 7. Power spectral density of the bear species studied. The dashed lines indicate the range of the measured papillae sizes across all species and the solid line indicates the wavevector of the melt layer between the polar bear paw pad and compressed snow (discussed later in the text). Error bars represent the standard error.

surface replicas (0.1 µm), it is not known how their area ratio compares with the other species when all length scales are included (down to angstrom level).

The friction stress results of our model surfaces on snow show that the friction stress is proportional to the ratio of the height divided by the diameter of the surface structures. However, a slip mode dominates at lower ratios, a fracture mode dominates at higher ratios, and a mixed mode is seen in the middle. In a pure slip mode, it is likely that it is the true contact area that governs the frictional stress [57]. In a pure fracture mode, it is likely that the cross-sectional area would dictate the stress (figure 11) [58,59]. Because both the true surface area and cross-sectional area of the model surfaces are proportional to H/D (electronic supplementary material, figure S2B), our results do not show a change in scaling at the mixed mode range.

One of the most complicating aspects of friction on snow or ice is that it is often near its melting temperature. In this case, once a paw pad is in contact with the snow, radiated heat will begin to melt some of the snow. We estimate that during a single step, heat from the paw pad will melt a layer of snow about $h_{melt} \approx 0.435$ µm thick, as depicted in figure 11. This melted layer will cover up all roughness with height less than h_{melt}, which corresponds to all roughness above the wavevector of $q_{melt} = 5.9 \times 10^6$ m^{-1} for the polar bear, with similar values for the other species (calculations in electronic supplementary material). At roughness above q_{melt}, the slope of the polar bear paw pad PSD amplitude decreases, while it shows no change for the brown and black bears (figure 7). Additionally, brown bears and black bears appear to continue to increase their area ratio (positive slope in figure 9) above q_{melt}, while the area ratio of the polar bear paw pad appears to remain constant (near zero slope). This shows that the smaller scale roughness, which does not play a role in contact with snow, is much smaller on the polar bear's paw pad than the brown and black bears'.

In the pure slip mode between a paw pad and snow, the maximum shear frictional stress is proportional to the true contact area. Because the melted layer covers all roughness at length scales above q_{melt}, those length scales do not contribute to an increased true contact area. Thus, for a pure slip mode, the relative frictional stress on snow for each species is proportional to the ratios of the true surface area ratios at each species' respective q_{melt}. This predicts that, in pure slip mode, the friction stress of a polar bear paw pad on snow will be 1.33 ± 0.03 times larger than that of the brown and black bear. Because the true surface area ratio is independent of paw pad size, this prediction is for both average-sized paws and paws scaled to the same size. For the pure fracture mode, it is the cross-sectional area that is proportional to the frictional stress. In this case, the cross-sectional area is proportional to $h_{pap}/D_{pap} \propto h_{rms}/D_{pap}$. When the paws are scaled to the same size, D_{pap} is constant for the three species, while h_{rms} is 1.50 ± 0.08 higher for the polar bear than the brown and black bear. Because the snow will be compressed to similar pressures for adults of all three bear species, and thus densities [60], the mechanical properties of the snow beneath the paw pad of each species will be similar [61] (see electronic supplementary material). This leads to the prediction that, in pure fracture mode, the friction stress of a polar bear paw pad on snow will be 1.50 ± 0.08 times larger than that of the brown and black bear. For a mixed failure mode between a paw pad and snow, the relative frictional stress is in between that of the slip and fracture modes. Thus, our final prediction is that, when scaled to the same size paws, the polar bear paw pad will produce a frictional stress on snow that is 1.33–1.50 times higher than that of the brown and black bears'.

With this prediction of the frictional stress of the paw pads on snow, and the measurement of the relative paw pad areas, it is possible to calculate an estimated frictional force for the entire paw pad by multiplying the relative frictional stress (1.33–1.50 × larger for the polar bear) by the relative paw pad area (1.7 × smaller). This estimates that for paws of the same size, the polar bear paw pad provides an upper limit of 0.9 ± 0.1 times as much frictional force on snow as its closest relatives. The polar bear paw pads are smaller, but the increased surface roughness on their paw pads contributes to a frictional force on snow that is nearly the same as that of the larger paw pads of the brown and black bear. As such, the increase in frictional shear stress theoretically induced by taller papillae does not appear to translate into improved frictional performance of a polar bear paw pad on snow in an absolute sense. Instead, our results suggest that taller papillae may compensate for frictional losses of a smaller paw pad, which has been suggested to conserve heat loss in this Arctic species [37].

Of course, our discussion only accounts for the surface roughness of paw pads. Other paw pad characteristics, such as surface chemistry and modulus, and other gross paw characteristics, such as fur and claws, will undoubtedly play a role in determining the whole organism friction on various substrates. Thus, until each of these variables is studied, this estimation should only be used in the context of isolating the paw pad surface roughness. Additionally, these results are most applicable to adult organisms. Younger organisms may produce different results due non-scalable growth of the papillae, paws and paw pads, and organism weights.

While our discussion is focused on the substrate of snow, there may be factors of the polar bear paw pad that are specifically adapted to ice. Because seawater contains salt, its presence on the ice will change its adhesion [62] and friction [63] properties compared with pure water and ice. These

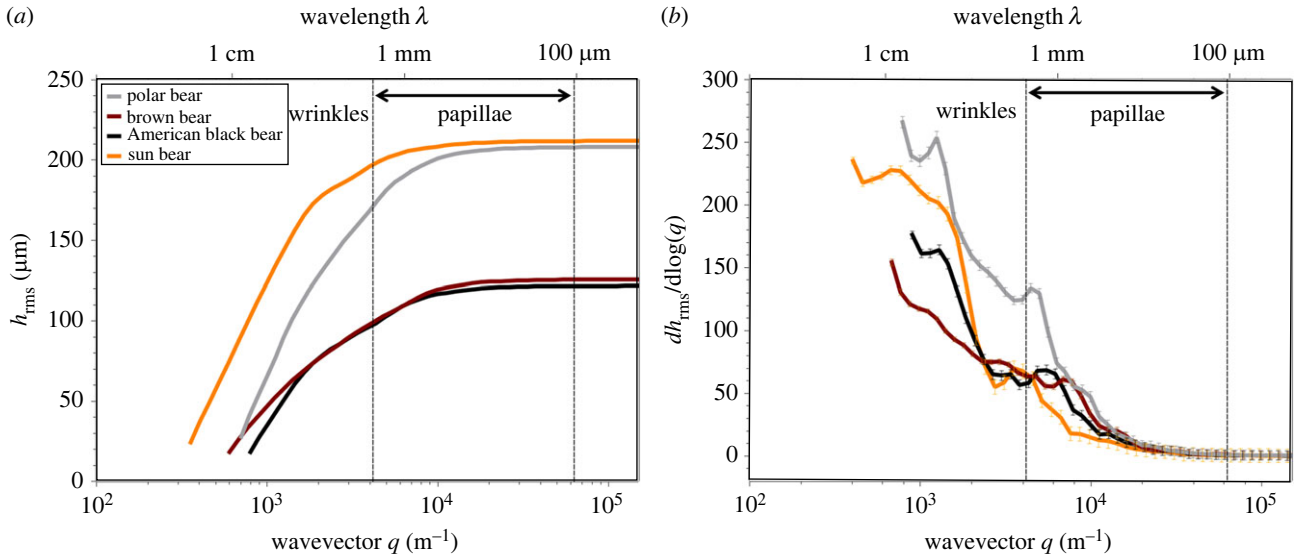

Figure 8. The cumulative root-mean-square average height as a function of the maximum wavevector included of the bear species studied (*a*). The slope of this function shows the contribution from roughness at each wavevector (*b*). The dashed lines indicate the range of the measured papillae sizes across all species. Note the abbreviated horizontal axis compared with figures 7 and 9. Error bars represent the standard error.

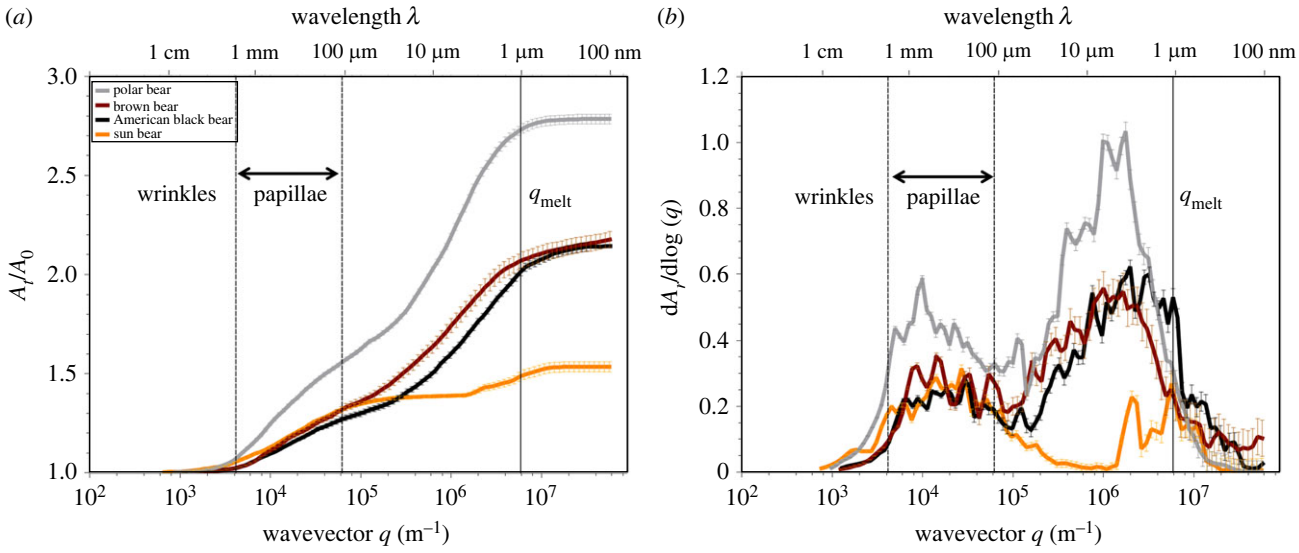

Figure 9. The cumulative true area ratio as a function of the maximum wavevector included of the bear species studied (*a*). The slope of this function shows the contribution from roughness at each wavevector (*b*). The dashed lines indicate the range of the measured papillae sizes across all species and the solid line indicates the wavevector of the melt layer between the paw pad and compressed snow. Error bars represent the standard error.

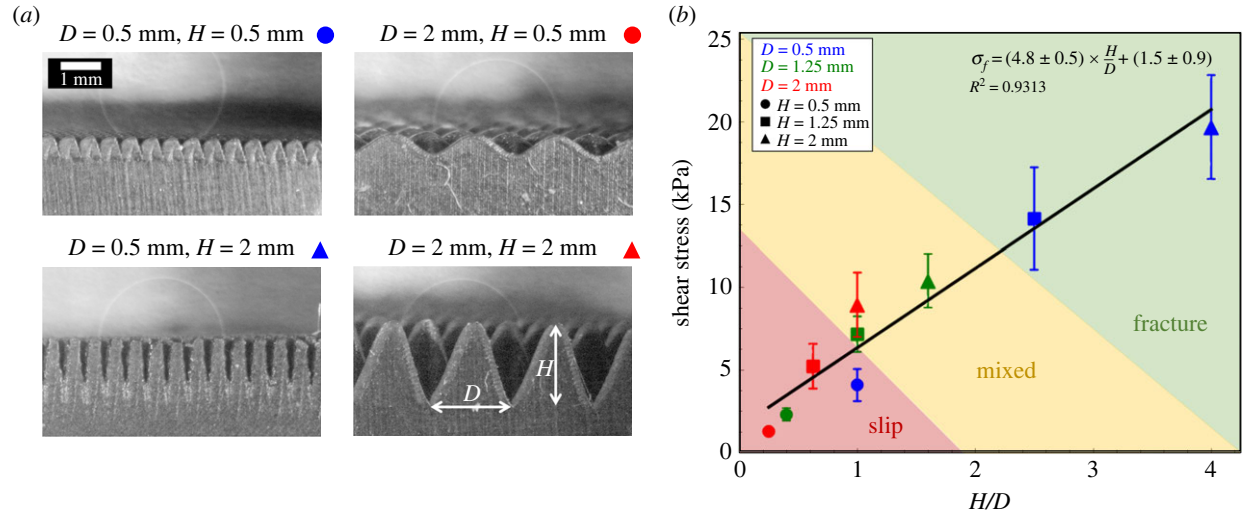

Figure 10. Optical microscopy images of the model surfaces with the smallest and largest papillae heights and diameters (*a*). The friction force between the model surfaces and snow is proportional to the aspect ratio of the papillae on the surface and show different modes of interfacial failure (*b*).

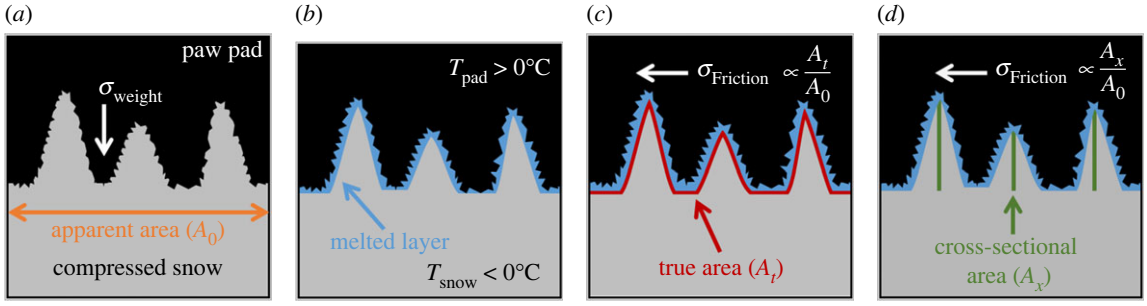

Figure 11. Proposed mechanisms for paw pad friction on snow. The snow is compressed into the paw pad roughness by the weight of the organism, creating complete contact (*a*). Heat from the paw pad melts a thin layer of snow, which covers the smaller length scales of roughness (*b*). In order for interfacial failure to occur, the paw pad must slip over the true contact area (*c*), fracture through the cross-sectional area (*d*), or a combination of both.

factors may further complicate prediction of relative friction on ice. There are probably also aspects of the paw pad surface roughness on different species that have adapted for enhanced performance on substrates in other habitats. This analysis is valid for any substrate that will take the shape of the paw pad surface roughness; however, the upper cut-off wavevector will be different for each substrate. The observation that scansorial sun bears and black bears have much more wrinkled paw pads than terrestrial polar bears and brown bears suggests that wrinkles aid in climbing, perhaps specifically to grip around tree branches. Other than the polar bear, bear species encounter several various substrates in their habitats, so similar studies for other species and substrates may be difficult.

5. Summary and conclusion

Previous studies found qualitative differences in bear paw morphology based on their habitat (e.g. claw length, amount of fur and size of paw pads) [28,64]. The only known study which examined the paw pad roughness of any bear species reported that polar bears have paw pad papillae of about 1 mm diameter, which were suggested to be adaptations for increased grip on snow and ice [26]. We have shown that although the larger base diameter of papillae of polar bears can be explained by a larger paw pad width, the papillae are 1.50 ± 0.08 times taller than those of the other species with similar paw pad widths. The taller papillae, and higher amplitude of roughness on the papillae, creates 1.33 ± 0.03 more true contact area between the polar bear paw pad and snow than that of the American black and brown bears. These results suggest that the maximum shear friction stress between a polar bear paw pad and snow is 1.33–1.50 times higher than American black and brown bear paw pads when their paws are scaled to the same size of the polar bear's. Considering the whole polar bear, the effect of the increased roughness on traction on snow nearly compensates for the decrease in traction due to smaller paw pads for minimizing thermal loss. Additionally, paw pad roughness on smaller length scales, which do not contribute to contact with snow, have a smaller amplitude on polar bears than the other species. The presence of wrinkles on the paw pads of scansorial sun bears and American black bears suggests that wrinkles may improve climbing performance, but future work is needed to validate this. Further comparative morphological and biomechanical studies in larger phylogenetic contexts will result in a more complete understanding of how paw pad surface roughness correlates with locomotor performance and habitat use.

Ethics. No animals were harmed or euthanized for the purposes of this study. Paw pad tissue from a polar bear (UAM:Mamm:138220) which died of unknown causes and a black bear (UAM:Mamm:138221) which died from natural causes was obtained from The University of Alaska's Museum of the North and used with the museum's permission. Paw pad tissue from a different black bear was obtained from Images Taxidermy (Newbury, OH 44065, USA) which was harvested by hunting under local regulations in October 2020 (2020 NJF&W Bear Tag no. 0000090) and used with permission. The remaining samples we made via surface replicas of taxidermized paws (i.e. no tissue was used for the study) with permission from the owners. Taxidermized paws of a sun bear which died from natural causes at the Akron Zoo (Akron, OH, USA) were used. The taxidermized animals observed in private collections were collected and/or purchased in accordance with all US federal and state laws. All experimental procedures were performed in accordance with The University of Akron's policies.

Data accessibility. The data are provided in electronic supplementary material [65].

Authors' contributions. N.O.: conceptualization, data curation, formal analysis, funding acquisition, investigation, methodology, project administration, validation, visualization, writing—original draft, writing—review and editing; A.M.G.: conceptualization, investigation, methodology, writing—review and editing; A.D.: funding acquisition, project administration, writing—review and editing.

All authors gave final approval for publication and agreed to be held accountable for the work performed therein.

Conflict of interest declaration. We declare we have no competing interests.

Funding. Funding was provided by NSF DMR 1610483 and the project was partially funded by a Goodyear Tire and Rubber Company Fellowship.

Acknowledgements. The authors thank the museum curators and the private taxidermists and collectors for access to samples, and Dr Michael C. Wilson for valuable discussions on the planning and background of the study.

References

1. Maderson PFA. 1964 Keratinized epidermal derivatives as an aid to climbing in gekkonid lizards. *Nature* **203**, 780–781. (doi:10.1038/203780a0)
2. Ruibal R, Ernst V. 1965 The structure of the digital setae of lizards. *J. Morphol.* **117**, 271–293. (doi:10.1002/jmor.1051170302)
3. Williams EE, Peterson JA. 1982 Convergent and alternative designs in the digital adhesive pads of scincid lizards. *Science*

215, 1509–1511. (doi:10.1126/science.215.4539.1509)

4. Autumn K, Liang YA, Hsieh ST, Zesch W, Chan WP, Kenny TW, Fearing R, Full RJ. 2000 Adhesive force of a single gecko foot-hair. *Nature* **405**, 681–685. (doi:10.1038/35015073)
5. Autumn K *et al.* 2002 Evidence for van der Waals adhesion in gecko setae. *Proc. Natl Acad. Sci. USA* **99**, 12252–12256. (doi:10.1073/pnas.192252799)
6. Russell AP. 2002 Integrative functional morphology of the gekkotan adhesive system (Reptilia: Gekkota). *Integr. Comp. Biol.* **42**, 1154–1163. (doi:10.1093/icb/42.6.1154)
7. Huber G, Mantz H, Spolenak R, Mecke K, Jacobs K, Gorb SN, Arzt E. 2005 Evidence for capillarity contributions to gecko adhesion from single spatula nanomechanical measurements. *Proc. Natl Acad. Sci. USA* **102**, 16 293–16 296. (doi:10.1073/pnas.0506328102)
8. Autumn K. 2006 How gecko toes stick. *Am. Sci.* **94**, 124–132. (doi:10.1511/2006.58.124)
9. Izadi H, Stewart KM, Penlidis A. 2014 Role of contact electrification and electrostatic interactions in gecko adhesion. *J. R. Soc. Interface* **11**, 2–5. (doi:10.1098/rsif.2014.0371)
10. Singla S, Jain D, Zoltowski CM, Voleti S, Stark AY, Niewiarowski PH, Dhinojwala A. 2021 Direct evidence of acid-base interactions in gecko adhesion. *Sci. Adv.* **7**, eabd9410. (doi:10.1126/sciadv.abd9410)
11. Barnes WJP, Oines C, Smith JM. 2006 Whole animal measurements of shear and adhesive forces in adult tree frogs: insights into underlying mechanisms of adhesion obtained from studying the effects of size and scale. *J. Comp. Physiol. A Neuroethol. Sensory, Neural, Behav. Physiol.* **192**, 1179–1191. (doi:10.1007/s00359-006-0146-1)
12. Federle W, Barnes WJ, Baumgartner W, Drechsler P, Smith JM. 2006 Wet but not slippery: boundary friction in tree frog adhesive toe pads. *J. R. Soc. Interface* **3**, 689–697. (doi:10.1098/rsif.2006.0135)
13. Endlein T *et al.* 2013 Sticking like sticky tape: tree frogs use friction forces to enhance attachment on overhanging surfaces. *J. R. Soc. Interface* **10**, 20120838. (doi:10.1098/rsif.2012.0838)
14. Langowski JK, Dodou D, Kamperman M, Leeuwen JL. 2018 Tree frog attachment: mechanisms, challenges, and perspectives. *Front. Zool.* **15**, 1–21. (doi:10.1186/s12983-018-0273-x)
15. Gorb S, Beutel R. 2001 Evolution of locomotory attachment pads of hexapods. *Naturwissenschaften* **88**, 530–534. (doi:10.1007/s00114-001-0274-y)
16. Gorb EV, Gorb SN. 2002 Attachment ability of the beetle *Chrysolina fastuosa* on various plant surfaces. *Entomol. Exp. Appl.* **105**, 13–28. (doi:10.1046/j.1570-7458.2002.01028.x)
17. Federle W. 2006 Why are so many adhesive pads hairy? *J. Exp. Biol.* **209**, 2611–2621. (doi:10.1242/jeb.02323)
18. Gorb SN. 2008 Biological attachment devices: exploring nature's diversity for biomimetics. *Phil. Trans. R. Soc. A* **366**, 1557–1574. (doi:10.1098/rsta.2007.2172)
19. Bullock JM, Federle W. 2009 Division of labour and sex differences between fibrillar, tarsal adhesive pads in beetles: effective elastic modulus and attachment performance. *J. Exp. Biol.* **212**, 1876–1888. (doi:10.1242/jeb.030551)
20. Bullock JM, Federle W. 2011 The effect of surface roughness on claw and adhesive hair performance in the dock beetle *Gastrophysa viridula*. *Insect Sci.* **18**, 298–304. (doi:10.1111/j.1744-7917.2010.01369.x)
21. Santos R, Hennebert E, Coelho A.2009 The echinoderm tube foot and its role in temporary underwater adhesion. In *Functional surfaces in biology* (ed. SN Gorb), pp. 9–41. Dordrecht, The Netherlands: Springer.
22. Dodou D, Breedveld P, De Winter JC, Dankelman J, Van Leeuwen JL. 2011 Mechanisms of temporary adhesion in benthic animals. *Biol. Rev.* **86**, 15–32. (doi:10.1111/j.1469-185X.2010.00132.x)
23. Wainwright D, Kleinteich T, Summers A. 2011 These dead fish really suck: adhesion performance of the northern clingfish. In *Society for Integrative and Comparative Biology 2012 Annual Meeting*. See https://sicb.org/abstracts/these-dead-fish-really-suck-adhesion-performance-of-the-northern-clingfish/.
24. Wainwright DK, Kleinteich T, Kleinteich A, Gorb SN, Summers AP. 2013 Stick tight: suction adhesion on irregular surfaces in the northern clingfish. *Biol. Lett.* **9**, 1–5. (doi:10.1098/rsbl.2013.0234)
25. Ditsche P, Summers AP. 2014 Aquatic versus terrestrial attachment: water makes a difference. *Beilstein J. Nanotechnol.* **5**, 2424–2439. (doi:10.3762/bjnano.5.252)
26. Manning DP, Cooper JE, Stirling I, Jones CM, Bruce M, McCausland PC. 1985 Studies on the footpads of the polar bear (*Ursus maritimus*) and their possible relevance to accident prevention. *J. Hand Surg. Am.* **10**, 303–307. (doi:10.1016/S0266-7681(85)80049-8)
27. *Paws have non-slip grip: Polar bear - AskNature*. https://asknature.org/strategy/paws-have-non-slip-grip/.
28. Pocock RI. 1914 On the feet and other external features of the Canidae and Ursidae. *Proc. Zool. Soc. Lond.* **84**, 913–941. (doi:10.1111/j.1469-7998.1914.tb07068.x)
29. Stirling I. 1990 *Polar bears*. Ann Arbor, MI: University of Michigan Press.
30. *Polar Bear Characteristics: Fur, Skin, Paws, Claws, and Weight - Polar Bears International*. https://polarbearsinternational.org/polar-bears/characteristics/.
31. Brown G. 1993 *Great bear almanac*. New York, NY: Lyons and Burford.
32. Kumar V, Lammers F, Bidon T, Pfenninger M, Kolter L, Nilsson MA, Janke A. 2017 The evolutionary history of bears is characterized by gene flow across species. *Sci. Rep.* **7**, 1–10. (doi:10.1038/srep46487)
33. Herrero S. 1972 Aspects of evolution and adaptation in American black bears (*Ursus americanus* Pallas) and brown and grizzly bears (*U. arctos* Linné.) of North America. *Bears Their Biol. Manag.* **2**, 221–231. (doi:10.2307/3872586)
34. Lee DC, Powell VJ, Lindsell JA. 2019 Understanding landscape and plot-scale habitat utilisation by Malayan sun bear (*Helarctos malayanus*) in degraded lowland forest. *Acta Oecologica* **96**, 1–9. (doi:10.1016/j.actao.2019.02.002)
35. Sasaki M *et al.* 2005 Adaptation of the hindlimbs for climbing in bears. *Ann. Anat.* **187**, 153–160. (doi:10.1016/j.aanat.2004.10.001)
36. Van Valkenburgh B. 1987 Skeletal indicators of locomotor behavior in living and extinct carnivores. *J. Vertebr. Paleontol.* **7**, 162–182. (doi:10.1080/02724634.1987.10011651)
37. Oritsland NA, Lentfer JW, Ronald K. 1974 Radiative surface temperatures of the polar bear. *J. Mammal.* **55**, 459–461. (doi:10.2307/1379018)
38. Renous A, Gasc JP, Abourachid A. 1998 Kinematic analysis of the locomotion of the polar bear (*Ursus maritimus*, Phipps, 1774) in natural and experimental conditions. *Netherlands J. Zool.* **48**, 145–167. (doi:10.1163/156854298x00156)
39. Davis BW, Li G, Murphy WJ. 2010 Supermatrix and species tree methods resolve phylogenetic relationships within the big cats, *Panthera* (Carnivora: Felidae). *Mol. Phylogenet. Evol.* **56**, 64–76. (doi:10.1016/j.ympev.2010.01.036)
40. Underwood LS, Reynolds P. 1980 Photoperiod and fur lengths in the arctic fox (*Alopex lagopus* L.). *Int. J. Biometeorol.* **24**, 39–48. (doi:10.1007/BF02245540)
41. Prestrud P. 1991 Adaptations by the arctic fox (*Alopex lagopus*) to the polar winter. *Arctic* **44**, 132–138. (doi:10.14430/arctic1529)
42. Klir JJ, Heath JE. 1992 An infrared thermographic study of surface temperature in relation to external thermal stress in three species of foxes: the red fox (*Vulpes vulpes*), Arctic fox (*Alopex lagopus*), and kit fox (*Vulpes macrotis*). *Physiol. Zool.* **65**, 1011–1021. (doi:10.1086/physzool.65.5.30158555)
43. Kumar V, Kutschera VE, Nilsson MA, Janke A. 2015 Genetic signatures of adaptation revealed from transcriptome sequencing of Arctic and red foxes. *BMC Genomics* **16**, 585. (doi:10.1186/s12864-015-1724-9)
44. Pagano AM *et al.* 2018 Energetic costs of locomotion in bears: is plantigrade locomotion energetically economical? *J. Exp. Biol.* **221**, jeb175372. (doi:10.1242/jeb.175372)
45. Mattson DJ. 2003 Foot loadings and pad and track widths of Yellowstone grizzly bears. *West. North Am. Nat.* **63**, 72–79.
46. Shine CL, Penberthy S, Robbins CT, Nelson OL, McGowan CP. 2015 Grizzly bear (*Ursus arctos horribilis*) locomotion: gaits and ground reaction forces. *J. Exp. Biol.* **218**, 3102–3109. (doi:10.1242/jeb.121806)
47. Shine CL, Robbins CT, Nelson OL, McGowan CP. 2017 Grizzly bear (*Ursus arctos horribilis*) locomotion: forelimb joint mechanics across speed in the sagittal and frontal planes. *J. Exp. Biol.* **220**, 1322–1329. (doi:10.1242/jeb.140681)
48. Iwaniuk AN, Pellis SM, Whishaw IQ. 2000 The relative importance of body size, phylogeny, locomotion, and diet in the evolution of forelimb dexterity in fissiped carnivores (Carnivora). *Can. J. Zool.* **78**, 1110–1125. (doi:10.1139/z00-023)
49. Murray DL, Larivière S. 2002 The relationship between foot size of wild canids and regional snow

conditions: evidence for selection against a high footload? *J. Zool.* **256**, 289–299. (doi:10.1017/S095283690200033X)

50. Takatsuki S. 1992 Foot morphology and distribution of Sika deer in relation to snow depth in Japan. *Ecol. Res.* **7**, 19–23. (doi:10.1007/BF02348593)
51. Murray DL, Boutin S. 1991 The influence of snow on lynx and coyote movements: does morphology affect behavior? *Oecologia* **88**, 463–469. (doi:10.1007/BF00317707)
52. Domine F, Sparapani R, Ianniello A, Beine HJ. 2004 The origin of sea salt in snow on Arctic sea ice and in coastal regions. *Atmos. Chem. Phys.* **4**, 2259–2271. (doi:10.5194/acp-4-2259-2004)
53. ASTM E112-13: Standard test methods for determining average grain size. *ASTM Int*. 2013. (doi:10.1520/E0112-13.1.4).
54. Orndorf N, Chen R-C, Work A. 2021 An investigation of the grain size and adhesion strength of high-speed impact ice. NASA/TM-20210014377.
55. Jacobs TD, Junge T, Pastewka L. 2017 Quantitative characterization of surface topography using spectral analysis. *Surf. Topogr. Metrol. Prop.* **5**, 013001. (doi:10.1088/2051-672X/aa51f8)
56. Dalvi S, Gujrati A, Khanal SR, Pastewka L, Dhinojwala A, Jacobs TDB. 2019 Linking energy loss in soft adhesion to surface roughness. *Proc. Natl Acad. Sci. USA* **116**, 25 484–25 490. (doi:10.1073/pnas.1913126116)
57. Persson BNJ. 2001 Theory of rubber friction and contact mechanics. *J. Chem. Phys.* **115**, 3840–3861. (doi:10.1063/1.1388626)
58. Weber B, Nagata Y, Ketzetzi S, Tang F, Smit WJ, Bakker HJ, Backus EH, Bonn M, Bonn D. 2018 Molecular insight into the slipperiness of ice. *J. Phys. Chem. Lett.* **9**, 2838–2842. (doi:10.1021/acs.jpclett.8b01188)
59. Liefferink RW, Hsia FC, Weber B, Bonn D. 2021 Friction on ice: how temperature, pressure, and speed control the slipperiness of ice. *Phys. Rev. X* **11**, 11025. (doi:10.1103/PhysRevX.11.011025)
60. Mellor M. 1977 Engineering properties of snow. *J. Glaciol.* **19**, 15–66. (doi:10.3189/s002214300002921x)
61. Petrovic JJ. 2003 Mechanical properties of ice and snow. *J. Mater. Sci.* **38**, 1–6. (doi:10.1023/A:1021134128038)
62. Orndorf N, Singla S, Dhinojwala A. 2020 Transition in the acid-base component of surface free energy of ice upon the premelting of its second molecular bilayer. *J. Phys. Chem. C* **124**, 19 588–19 594. (doi:10.1021/acs.jpcc.0c04610)
63. Roberts AD, Lane JD. 1983 Friction of rubber on ice in the presence of salt. *J. Phys. D. Appl. Phys.* **16**, 275–285. (doi:10.1088/0022-3727/16/3/011)
64. Pocock RI. 1918 Further notes on some external characters of the bears (Ursidae). *Ann. Mag. Nat. Hist.* **1**, 375–384. (doi:10.1080/00222931808562331)
65. Orndorf N, Garner AM, Dhinojwala A. 2022 Polar bear paw pad surface roughness and its relevance to contact mechanics on snow. Figshare. (doi:10.6084/m9.figshare.c.6260159)